

Influence of molar concentration on ethylene diamine tetra acetic acid (EDTA) added to tin sulfide (SnS) thin films grown by silar method

P. Mani¹ · K. Manikandan² · J. Joseph prince¹

Received: 21 November 2016 / Accepted: 22 May 2017 / Published online: 6 June 2017
© Springer Science+Business Media New York 2017

Abstract Nano thin films of SnS were prepared for solar cell application as absorber layer to analyse energy band gap. Thin films of Tin Sulphide (SnS) were deposited on glass substrate in room temperature by Successive Ionic Layer Adsorption and Reaction method. The changes in the properties of SnS were studied, when a complexing agent ethylenediaminetetraacetic acid (EDTA) added. The deposition parameters such as Dip duration is 35 s, Ex-dip duration is 5 s, Number of cycles are 25 and Number of dips are four were optimized to obtain good quality of SnS films. The Structural, morphological, topographical and optical properties of EDTA added Tin Sulphide thin films were characterized by X-ray diffraction (XRD), SEM, AFM, UV–Vis spectrometry and FT-IR techniques. The deposited SnS films are in amorphous and polycrystalline structure. The UV–Vis spectra of SnS films in the wavelength range of 200–900 nm have been observed to find the direct band gap. The band gap energy ($E_g = 2.31, 2.27, 2.16, 2.09$ eV) decreases with increase in molar concentration (0.05, 0.10, 0.15 and 0.20 M). Band gap decreases with increasing particle size.

1 Introduction

Thin films are used in opto-electronic devices and photo-conductive cells for their compactness, trouble-free coating

techniques and for their cost-effectiveness. Because of the large band gap and transparency in the visible region of Tin Sulfide, it is used as an absorber layer for solar cells, solar collectors and etc. SnS satisfy most of the criteria to make them prospective material in photoelectrochemical thin film solar cells for photovoltaic materials and in other optoelectronic systems [1]. Tin Sulfide thin films [1, 2] are deposited already by different techniques such as: electro deposition [3, 4], chemical bath deposition [5, 6], spray pyrolysis [7], electro chemical deposition [8], chemical deposition [9], pulse electro deposition [10], evaporated [11], co-evaporated [12], thermal evaporation [13], RF sputtering [14], vacuum-evaporation [15], colloidal synthesis [16] and SILAR [1, 17–26]. In the present research work, thin films of Tin Sulfide (SnS) with Ethylene Diamine Tetra Acetic acid $C_{10}H_{14}N_2Na_2O_8$ (EDTA) are deposited on glass substrate in room temperature by Successive Ionic Layer Adsorption and reaction (SILAR) method. In SILAR technique, several coatings of tin nitrate $[Sn(NO_3)_2]$ as cationic precursor and sodium sulfide (Na_2S) as anionic precursor are made.

Presence of complexing agents such as EDTA [2–6, 27–29] in the solution of metal chalcogenide thin films is found to improve the quality of the deposited films, such as the uniformity, crystallinity and the adhesion of the deposited film on the substrate [10]. The EDTA is used for making stable metal complexes; hence it is widely employed in analytical and industrial applications as a complexing agent for the wide spread of materials. Uncomplexed EDTA adsorbed quickly within a few minutes on the surface of glass plate [23]. The structural, morphological, topographical and optical properties of EDTA added tin sulfide thin films are characterized by X-ray diffraction (XRD), SEM, AFM, FT-IR and UV–Vis spectrometry techniques.

✉ P. Mani
maniprahaspathy@gmail.com

¹ Department of Physics, Anna University - BIT Campus,
Tiruchirappalli 620024, India

² Department of Physics, Bharathidasan University Constituent
Model Women's College, Veppur 621717, India

2 Experimental details

2.1 Preparation of SnS thin films with EDTA

Figure 1 shows the experimental set up of SILAR. The glass plates are degreased with acetone and rinsed by concentrated nitric acid. The glass plates rinsed with a detergent solution is washed with distilled water and dried in air. Tin sulfide thin films are prepared from the beakers containing aqueous solutions of tin nitrate $[\text{Sn}(\text{NO}_3)_2]$ and

sodium sulfide $[\text{Na}_2\text{S}]$. The tin nitrate and sodium sulfide are kept at 1:1 molar ratio of all the concentrations. 4 ml of EDTA is added to tin nitrate solution. Because EDTA can retard the deposition of Sn^{2+} through chelation, it is easier to obtain the stoichiometry SnS films with good quality by adding EDTA [5]. The film deposition process carried out with the following parameters are mentioned in Table 1. Pre-cleaned glass plates are immersed in cationic precursor tin nitrate for 35 s, so that Sn^{2+} ions present in the solution can be adsorbed on the glass plates. Then, the substrate is

Fig. 1 Schematic representations of SILAR deposition for SnS thin films with EDTA



Table 1 Deposition parameters in SILAR controller settings for SnS thin films with EDTA

Source of material	Tin nitrate	Distilled water	Sodium sulfide	Distilled water
Volume	100 ml	100 ml	100 ml	100 ml
Concentration	0.05–0.25 M	–	0.05–0.25 M	–
Temperature	31 °C	31 °C	31 °C	31 °C
Complexing agent	EDTA (4 ml)	NIL	NIL	NIL
Start position	0	0	0	0
Dip length	75 mm	75 mm	75 mm	75 mm
Dip speed	5 mm/s	5 mm/s	5 mm/s	5 mm/s
Retrieval speed	4 mm/s	4 mm/s	4 mm/s	4 mm/s
Dip duration	35 s	35 s	35 s	35 s
Ex. dip duration	4 s	4 s	4 s	4 s
No. of cycles	30	30	30	30
Soluble in	Dist. water	–	Dist. Water	–
Source of ions	Sn ²⁺	–	S ²⁻	–

rinsed in distilled water for 35 s, so that, the excessively adsorbed Sn²⁺ ions are removed away from the deposited layer which may result in saturated adsorbed layer of (Sn²⁺) cations on the glass plate. The cation coated films are immersed in anionic precursor for 35 s. It leads to reaction with the anions S²⁻ from the sodium sulfide solution and is introduced to the system. As a result of it, solid substrate is formed over the interface. Un-reacted sulfide ions are detached by immersing them in distilled water for 35 s. Thus, a SILAR cycle comprises these four parts. These operations were repeated for 30 SILAR cycles in order to get an adherent film (Fig. 1).

3 Results and discussion

3.1 XRD analysis

The X-ray diffraction patterns of the EDTA added SnS thin films deposited by SILAR technique in 0.20 and 0.25 M on glass substrates at room temperature are shown in Figs. 2 and 3. The inter atomic spacing (*d*), full width half maximum (β), average particle size (*D*), micro strain (ϵ) and dislocation density (ρ) values of EDTA added SnS thin film are calculated by using the data obtained from XRD analysis and tabulated in Tables 2 and 3.

The *d*-Spacing, average particle size, FWHM (β in Radian), dislocation density (ρ) and micro strain (ϵ) have been estimated by the following formulae,

$$2d \sin \theta = n\lambda \text{ (Bragg's Law)} \quad (1)$$

$$D = \frac{0.9\lambda}{\beta \cos \theta} \text{ (Using Debye-Scherrer formulae)} \quad (2)$$

$$\epsilon = \frac{\beta \cos \theta}{4} \text{ line/m}^2 \quad (3)$$

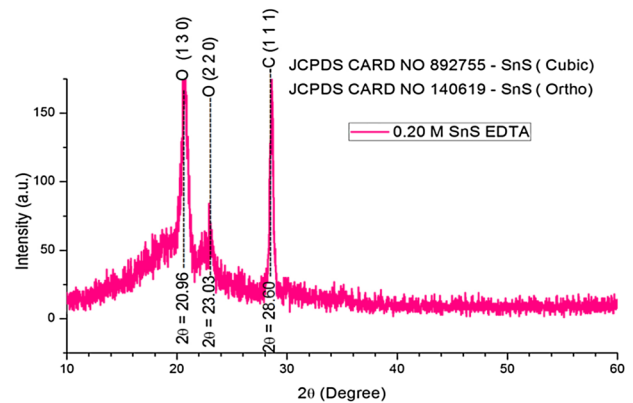


Fig. 2 XRD pattern of EDTA added SnS thin film in 0.20 M concentration. (Color figure online)

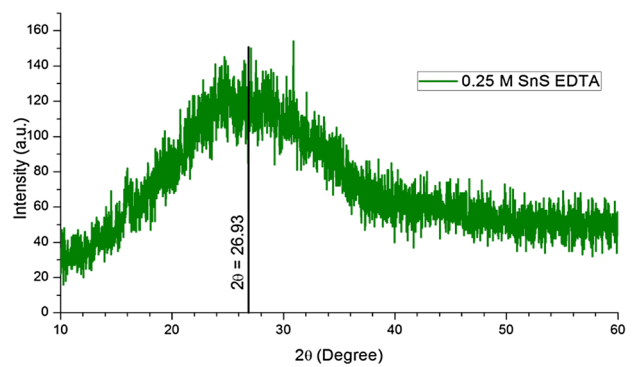


Fig. 3 XRD pattern of EDTA added SnS thin film in 0.25 M concentration. (Color figure online)

$$\rho = \frac{1}{D^2} \quad (4)$$

$$\beta = (\beta \text{ in Degree})\pi/180^\circ \text{ radian} \quad (5)$$

Table 2 Structural parameters of EDTA added SnS thin films in 0.20 and 0.25 M concentrations

SnS EDTA 0.20 M $\lambda=0.1546$ nm; $n=1$							
2θ (°)	h k l	'd' spacing Å	' β ' FWHM (°)	' β ' (Radian)	'D' (nm)	' ϵ ' $\times 10^{-3}$ line ² /m ⁻⁴	' ρ ' $\times 10^{-3}$ line/m ²
20.55	(1 3 0)	4.34	0.80	0.01396	10.56	8.968	3.434
22.85	(2 2 0)	4.282	0.60	0.01047	13.56	5.440	2.566
28.55	(1 1 1)	3.124	0.374	0.00652	22.00	2.066	1.581
SnS EDTA 0.25 M amorphous							

Table 3 The surface properties of SnS thin film with EDTA for 0.20 and 0.25 M in 5 and 10 μ m magnifications

0.20 M (d) & 0.25 M (e)	5 μ m			10 μ m		
	Grain size (Δx) (nm)	Surfaces roughness (Ra) (nm)	Surface height (Rz) (nm)	Grain size (Δx) (nm)	Surfaces roughness (Ra) (nm)	Surface height (Rz) (nm)
Min (d)	140	2.97	13.12	180	50.07	136.54
Max(d)	230	7.55	29.98	300	66.58	203.47
Min (e)	120	22.85	74.55	230	9.97	30.73
Max(e)	240	24.54	93.01	850	17.92	56.70

where λ is the wave length of X-rays (0.1546 nm), $n=1$ integer, d is interplanar spacing between the atoms, β is FWHM (full width at half maximum), ' θ ' is the diffraction angle and ' D ' is particle diameter, ρ is the dislocation density, and ϵ is micro strain. The XRD peaks are observed from 10° to 30° . The deposited films are found to have mixed orthorhombic and cubic phase for 0.20 M concentration and agree well with the standard data from JCPDS card Nos. 140619 and 892755 respectively. The observed d spacing and hkl planes values of orthorhombic (1 3 0) and (2 2 0) and cubic (1 1 1) phase for corresponding 2θ values are tabulated in Table 2. The intensity of the diffraction peak depend on the possible diffraction directions and the lattice parameters such as a , b and c in the phase of orthorhombic. The XRD pattern of EDTA added SnS thin film for 0.25 M a broad diffraction hump at $2\theta=26.93^\circ$ and expresses the amorphous nature of the film. The calculated value of micro strains and the dislocation density values are calculated as shown in the Table 2. These observations indicate that, the dislocation density and the microstrain of the films are found to decrease with increasing concentration. It has been observed that the crystalline properties and the crystallite size also increased with the increasing molar concentrations. Since, the dislocation density and the micro strain of the films are decreased with increasing concentrations, the crystalline nature and the crystallite sizes are enhanced. These observations infer that the crystalline properties are improved with the increase in concentrations.

3.2 SEM analysis

The surface of the EDTA added SnS (1:1) with different molar concentration of nano thin films are examined by Scanning Electron Microscope (SEM) at different magnification. The SEM micrographs for the different concentration films are represented in Fig. 4a–e. It can be noticed that the presence of EDTA in SnS film reveals that the SnS nano films are distorted layer in the surface of the thin films. Basically EDTA assists to create the complex of the Sn compound. Also it is confirmed that the influences of EDTA have significantly changed in the colour of the film. Particularly, the SEM images of 0.10 and 0.15 M concentration of EDTA has uniform and granular particle morphology with few crystals. For 0.05, 0.20 and 0.25 M the film coating is uniform with irregular shapes with small crystals. For 0.15, 0.20 and 0.25 M, in addition to the symmetric coating, there is a pearl like structure is also observed. It looks like the spots in the surface of the moon. It may be confirmed that the changing morphology of the films are strongly dependent on the increasing concentration of SnS. The SEM micrograph observed for all the films shows that the surface appears partially smooth with few isolated islands and minute pearl like particles over the surface.

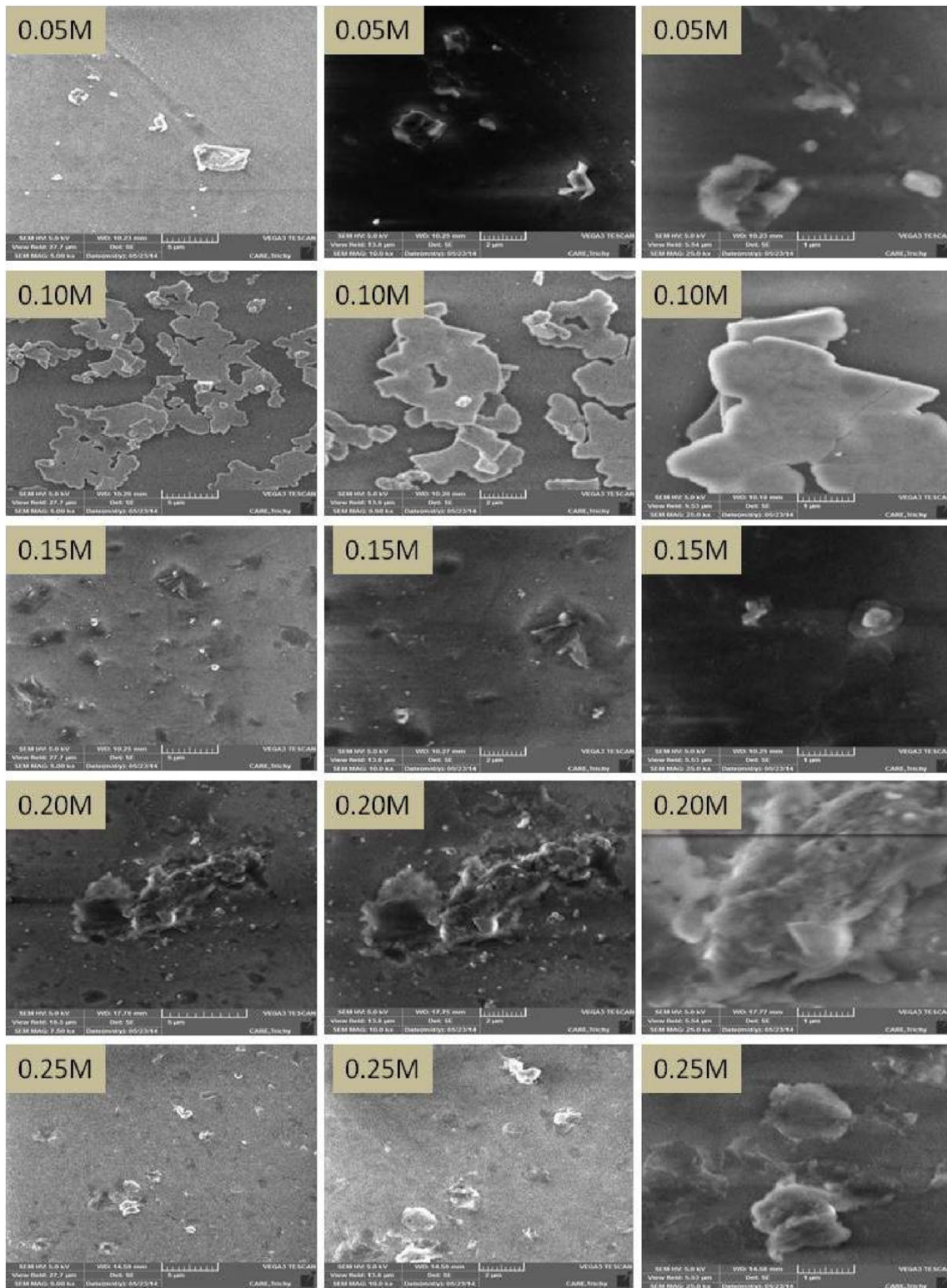


Fig. 4 SEM images of SnS thin films with EDTA for different molar concentrations in 5, 2 and 1 μm magnifications

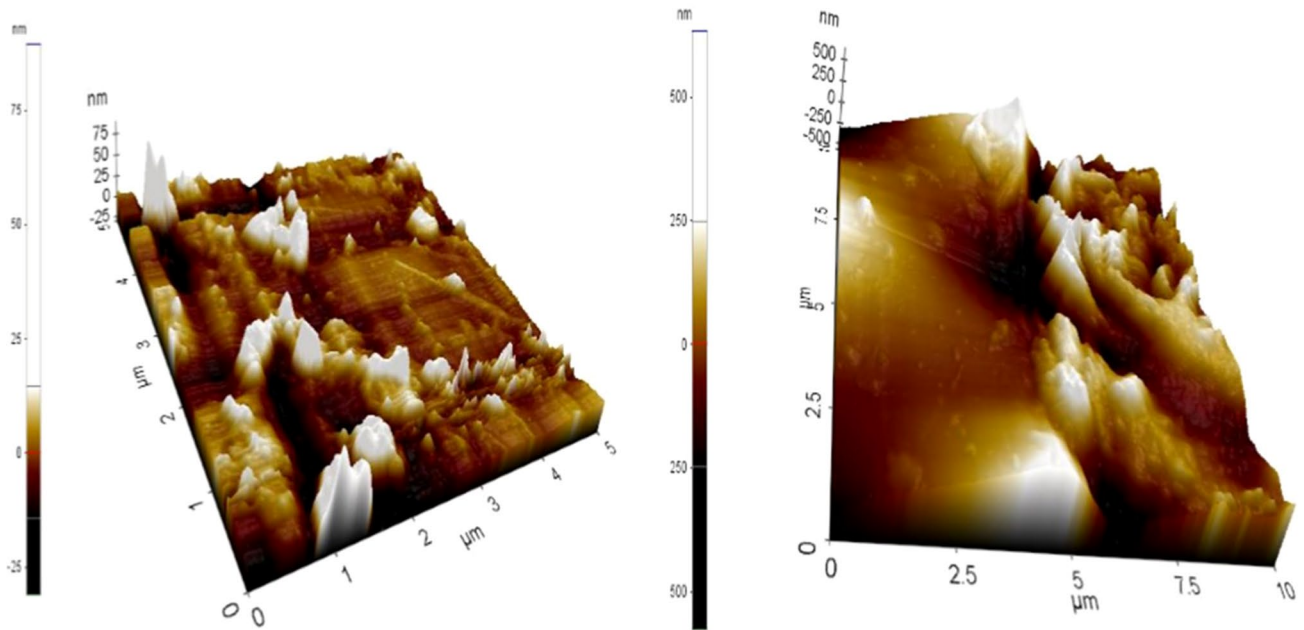


Fig. 5 3D AFM images of SnS thin films with EDTA of 0.20 M in 5 & 10 μm magnifications

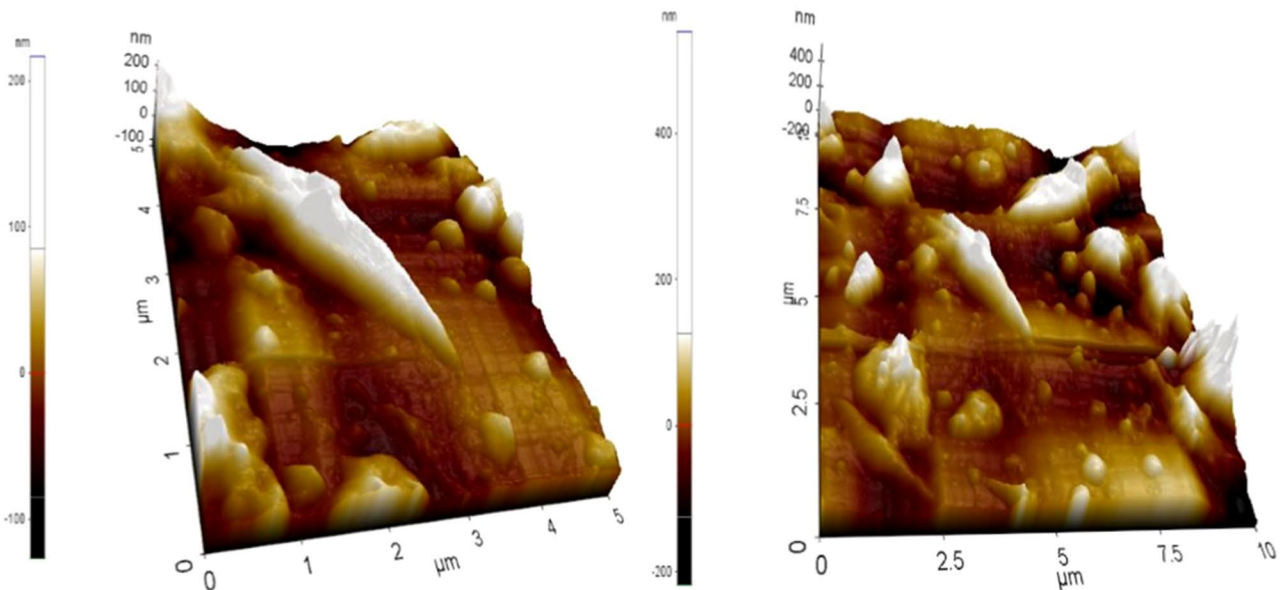


Fig. 6 3D AFM images of SnS thin films with EDTA of 0.25 M in 5 and 10 μm magnifications

3.3 AFM analysis

SnS thin films with complexing agent EDTA are investigated by Atomic Force Microscope (AFM) for its average roughness, particle height and for its grain size. The 3D and 2D AFM images of SnS thin films with EDTA of 0.20 and 0.25 M are recorded in 5 and 10 μm as shown in Figs. 5a, b, 6a, b, 7, 8, 9, 10. The scanned area

is focused for 10 μm . Red and green lines are drawn to observe the tabulated factors (Table 3). Significantly, the change in topography of the thin film is observed for two different magnifications. These images confirm the coating in full surface. Here, some particles are oriented in certain places with maximum height which is mentioned by white patterns. The rest of the maximum area reveals the minimum height of the particle which confirms the

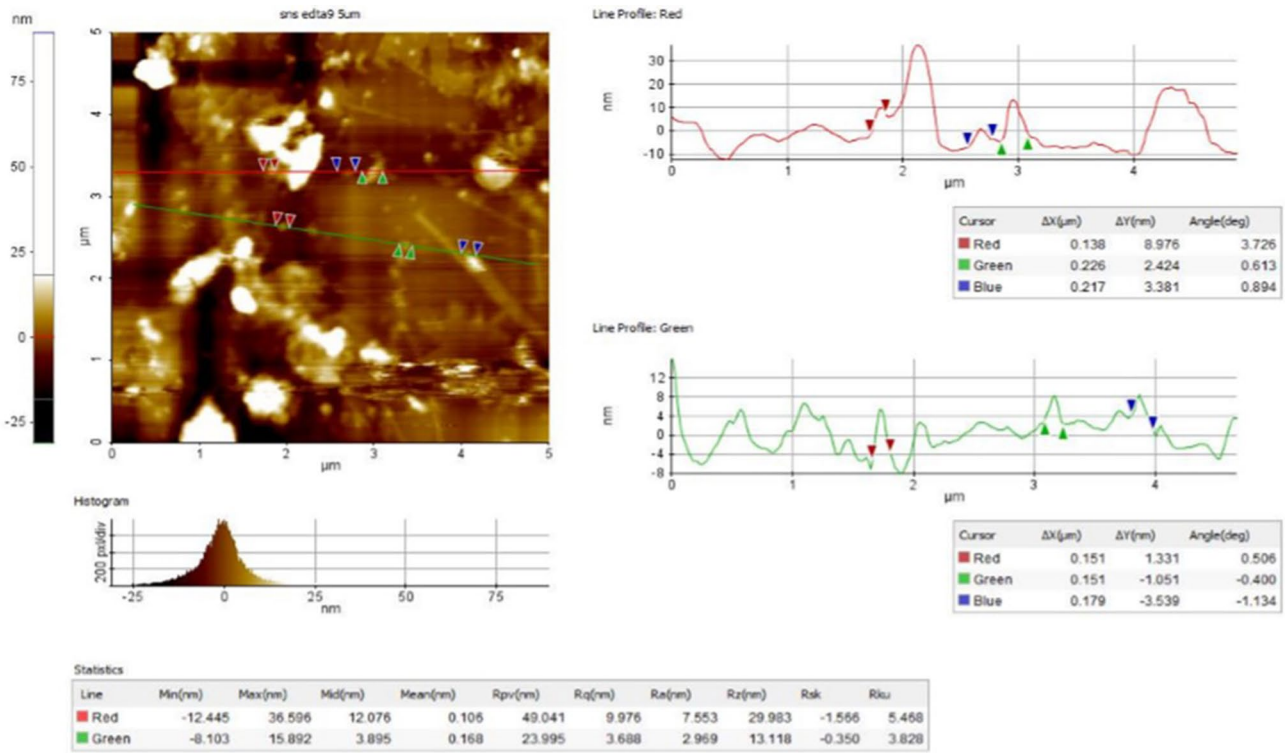


Fig. 7 2D AFM image of SnS thin film with EDTA of 0.20 M in 5 μm magnification. (Color figure online)

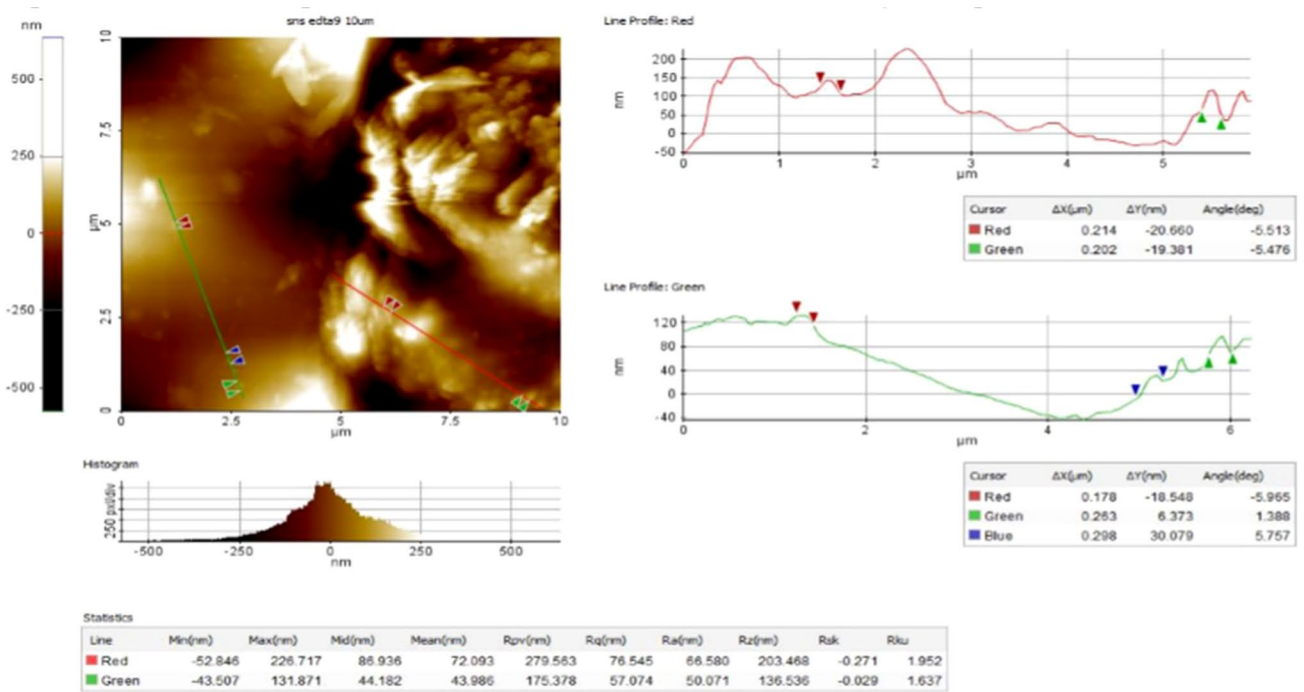


Fig. 8 2D AFM image of SnS thin film with EDTA of 0.20 M in 10 μm magnification. (Color figure online)

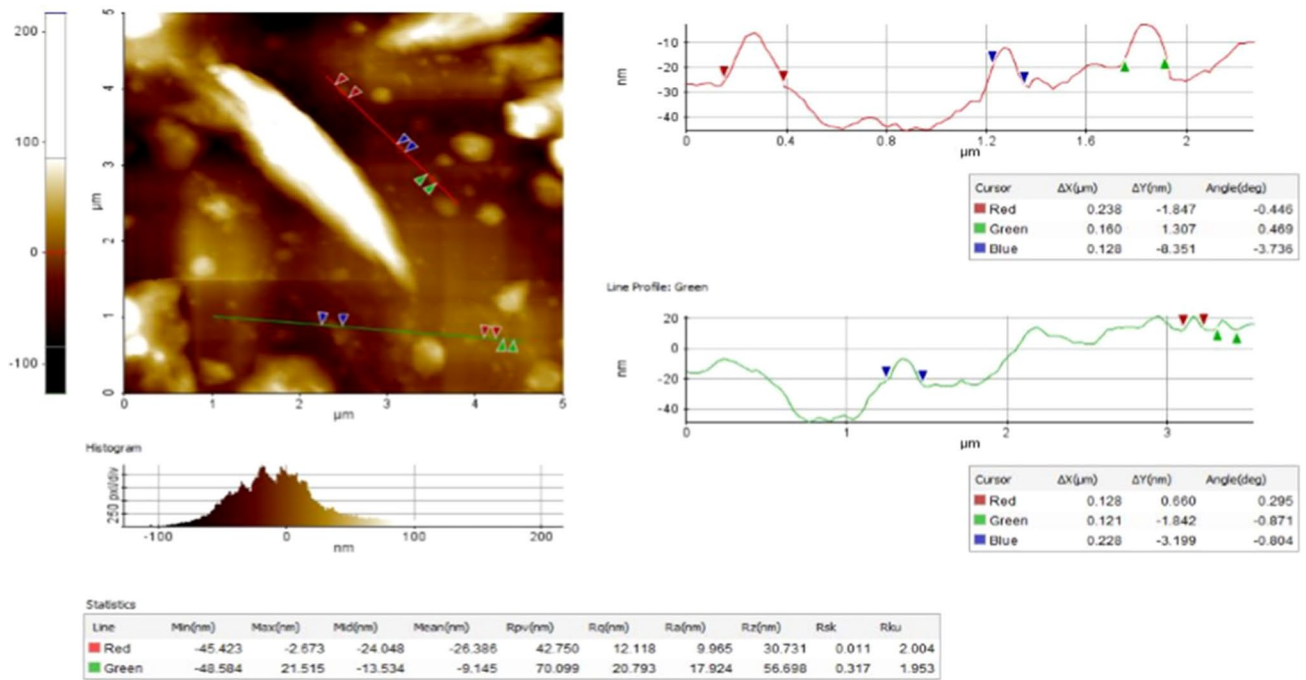


Fig. 9 2D AFM image of SnS thin film with EDTA of 0.25 M in 5 μm magnification. (Color figure online)

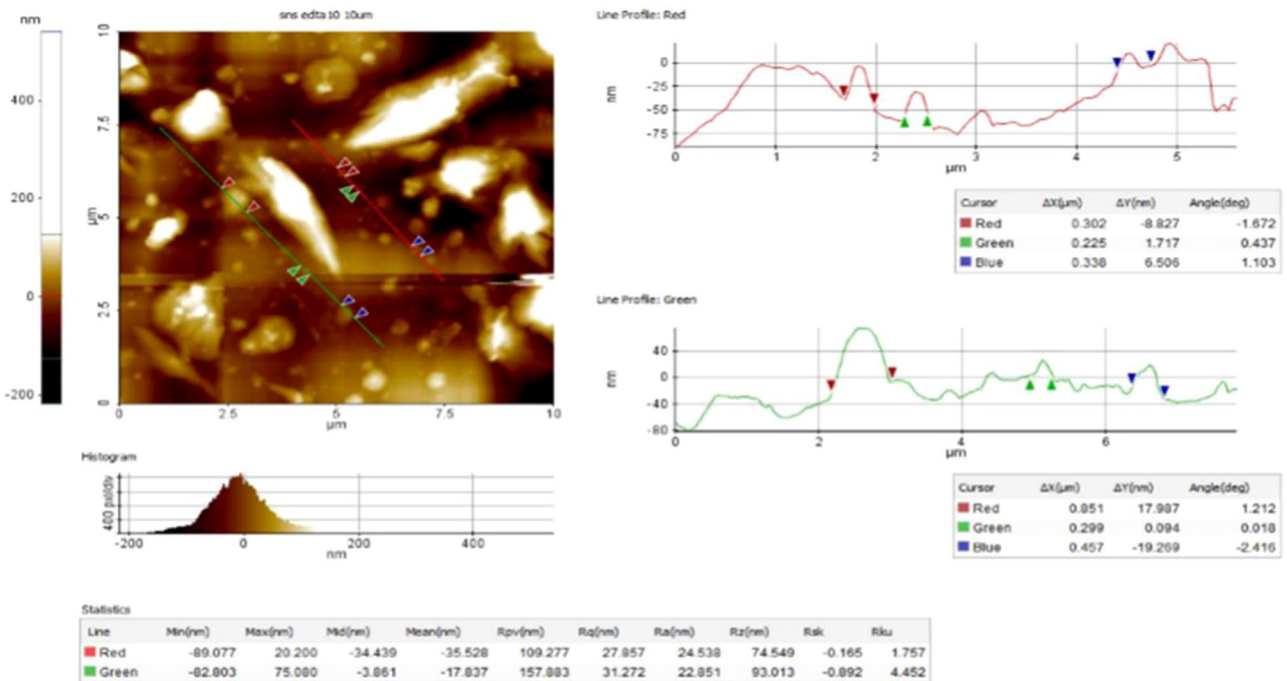


Fig. 10 2D AFM image of SnS thin film with EDTA of 0.25 M in 10 μm magnification. (Color figure online)

uneven surface. For the decreasing size of the particle, smoothness increases. The AFM images indicate these samples are found to cover the surface of the substrate entirely. The observed surface roughness, grain size and surface height are given in Table 3.

From the Table 3, it is confirmed that the roughness and the particle height are not uniform in 10 and 5 μm which shows the material is coated uniformly with irregular particle size. Even though particles are in different size, the smoothness of the surface in the coated film is

not affected. But the change in surface height may affect the smoothness. For 5 μm in 0.20 and 0.25 M, roughness is varying between 2.97 and 24.54 nm which confirms that the material is coated uniformly with the irregular particle size. i.e. the particle height varies from 13.12 to 93.01 nm. Minimum and maximum grain size (Δx) is observed to be 120 and 240 nm. Pits and peaks vary between -48.58 and 36.60 nm. For 10 μm in 0.20 and 0.25 M, roughness varies from 9.97 to 66.58 nm which confirms that the material is coated uniformly with the irregular particle size. i.e., the particle height varies from 30.73 to 203.47 nm. The grain size (Δx) observed is about 180 and 850 nm. Pits and peaks vary between -89.08 and 228.72 nm.

3.4 FT-IR analysis

The FT-IR spectra of EDTA added SnS thin films with different molar concentrations of 0.10, 0.15, 0.20 and 0.25 M are presented in Fig. 11. FT-IR measurements have been made in the wave number range 400–4000 cm^{-1} . A broad absorption peak between 3520 and 2910 cm^{-1} is assigned to O-H stretching vibration of the absorbed water in the sample. The presence of water is also confirmed by its bending vibration observed at 1977 cm^{-1} . A broad peak observed around 1977–818 cm^{-1} is possibly due to stretching vibrations of sulphate group. The absorption bands observed at 493 and 818 cm^{-1} are possibly due to Sn–S stretching vibration. These peaks are ascribed to the stretching vibration of Sn–S bonds, indicating the formation of SnS film [23, 30–32].

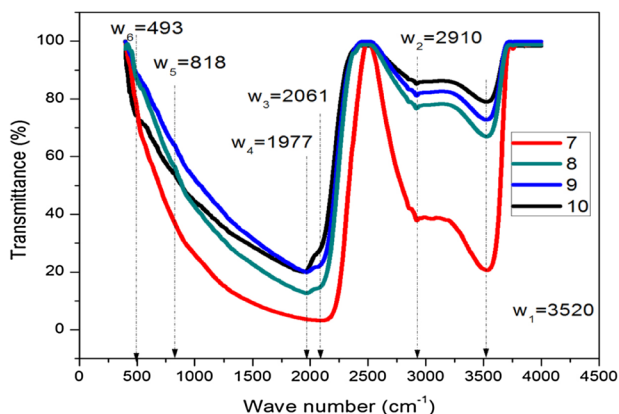


Fig. 11 FTIR spectra of EDTA added SnS thin films of (7) 0.10 M, (8) 0.15 M, (9) 0.20 M and (10) 0.25 M concentrations. (Color figure online)

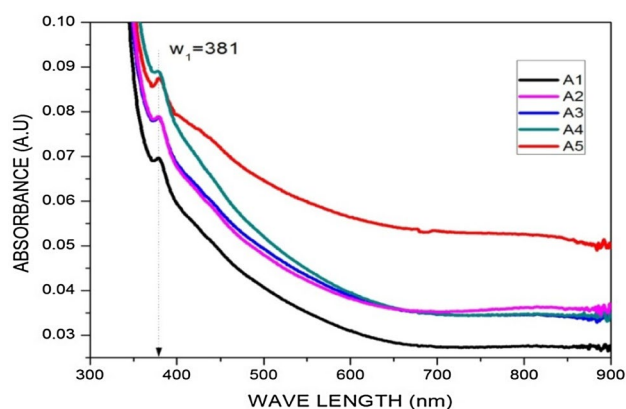


Fig. 12 Absorbance of EDTA added SnS thin films for A1 0.05 M; A2 0.10 M; A3 0.15 M; A4 0.20 M and A5 0.25 M. (Color figure online)

3.5 UV-Visible analysis

3.5.1 Optical absorbance analysis

The optical absorbance of the deposited films in the increasing concentration (0.05–0.25 M) has been studied in the wavelength range 300–800 nm. Figure 12 shows the UV-Vis absorption spectrum of EDTA added SnS thin film with various molar concentrations. From the Fig. 12 it is observed that the absorbance peak is at 381 nm wavelength invariantly for all the concentrations. The SnS with EDTA films are showing higher absorbance in the visible region, lower absorbance in the near-IR region and absorbance maintained as almost constant in IR region. The increasing absorbance is observed in the visible and IR regions with increasing molar concentrations. Photon is inducing more

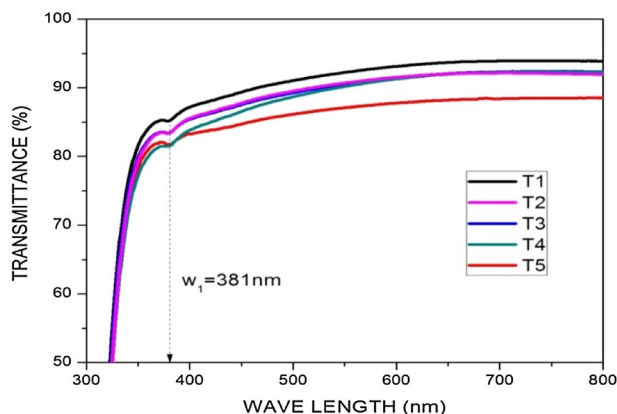


Fig. 13 Transmittance of EDTA added SnS thin films for T1 0.05 M, T2 0.10 M, T3 0.15 M, T4 0.20 M and T5 0.25 M. (Color figure online)

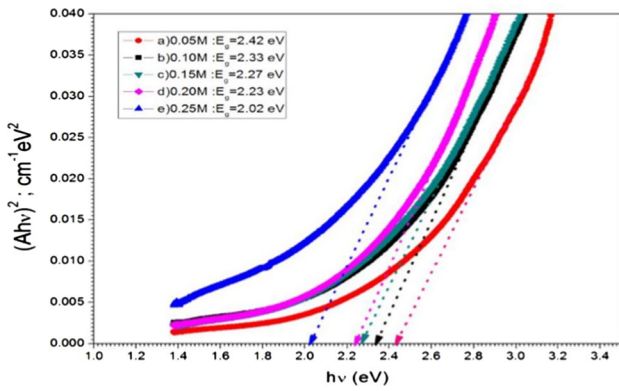


Fig. 14 Band gap analysis of EDTA added SnS films of (a) 0.05 M, (b) 0.10 M, (c) 0.15 M, (d) 0.20 M and (e) 0.25 M. (Color figure online)

number of electrons (from 650 to 700 nm) for the increasing molar concentrations.

3.5.2 Optical transmittance analysis

The transmittance spectrum is shown in Fig. 13. From the Fig. 13 it is confirmed that the transmission decreases with the increasing molar concentrations also it is observed that the transmission increases from visible region to IR region.

3.5.3 Band gap analysis

The band gap energy of the film has been determined by the extrapolation of the linear regions on the x axis ($h\nu$). From the Fig. 14, the band gap energy of the EDTA added SnS thin films of 0.05, 0.10, 0.15, 0.20 and 0.25 M are 2.42, 2.33, 2.27, 2.23 and 2.02 eV respectively. Thus, a plot of $(Ah\nu)^2$ versus $h\nu$ is a curved line. As the molar concentration increases, the band gap energy values decrease which may be due to the mobility of more number of electrons from the valence band to the conduction band. The particle size increases for the increasing molarity resulting in decreasing bandgap [22].

3.5.4 Influence of increasing molar concentration

Influence of increasing molar concentration on optical absorption, transmittance and band gap energy is shown in Fig. 15. Table 4 shows the comparative analysis on the effect of various molar concentration on optical properties of the deposited thin films. A comparative analysis of optical absorbance, transmittance and band gap is shown in Table 4. The effect of increasing molar concentration on optical absorbance, transmittance and band gap energy are given in Fig. 15. The optical absorbance of the deposited films increases (0.069–0.089 a.u.) with the increasing

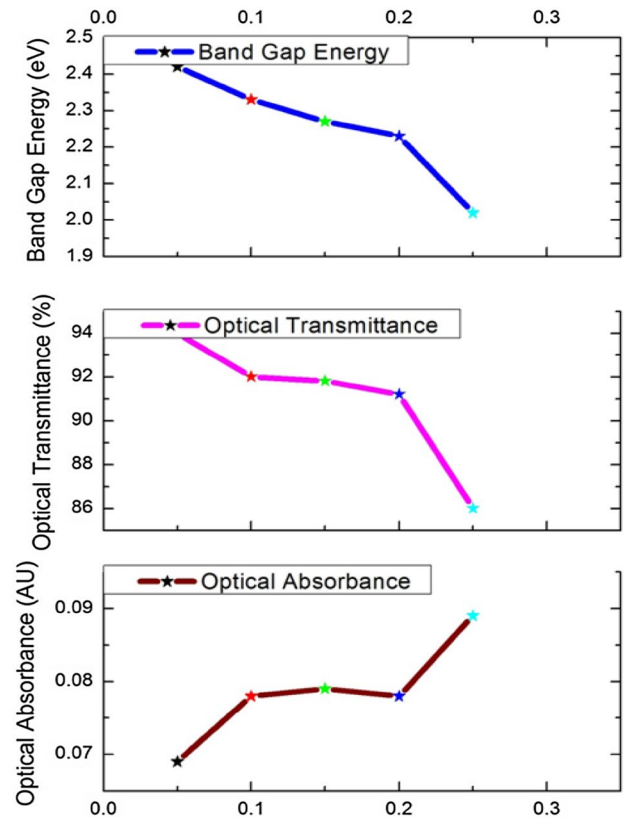


Fig. 15 Influence of increasing molar concentration on optical properties SnS thin films with EDTA. (Color figure online)

molar concentration (0.05–0.25 M). The optical transmittance (94–86%) of the deposited films is decreasing for the increasing concentration (0.05–0.25 M). Band gap energy is decreasing (2.42–2.02 eV) for the increasing concentration (0.05–0.25 M).

4 Conclusion

EDTA added tin sulfide thin films are deposited in different molar concentration using SILAR technique in room temperature. The inter atomic spacing (d), full width half maximum (β), average particle size (D), micro strain (ϵ) and dislocation density (ρ) values of EDTA added thin film are calculated by using the data obtained from XRD analysis. The deposited films are found to have mixed orthorhombic and cubic phase for 0.20 M concentration and agree well with the standard data from JCPDS card Nos. 140619 and 892755 respectively. The XRD pattern for 0.25 M a broad diffraction hump at $2\theta=26.93^\circ$ and expresses the amorphous nature of the film. FTIR spectrum confirms the various functional groups present in the deposited film. SEM image confirms that the changing morphology of the films are strongly dependent on the increasing

Table 4 Influence of molar concentration on optical properties SnS thin films with EDTA

Molar concentration (M)	Optical absorbance (a.u.)	Optical transmittance (%)	Band gap energy (eV)
0.05	0.069	94	2.42
0.10	0.078	92	2.33
0.15	0.079	91.8	2.27
0.20	0.078	91.2	2.23
0.25	0.089	86	2.02

concentration of SnS. AFM images confirm the coating in full surface of the substrate. The optical absorbance peak is observed at 381 nm. Transmittance decreases with increasing molar concentration in visible region. The band gap energy decreases from 2.42 to 2.02 eV for increasing molar concentration.

References

- P. Mani, K. Manikandan, J.J. Prince, *J. Mater. Sci. Mater. Electron.* **27**(1), 744 (2016)
- S. Cheng, Y. He, G. Chen, *Mater. Chem. Phys.* **110**, 449(2008)
- K. Jiang, Y. Wang, J. Dong, L. Gui, Y. Tang, *Langmuir (ACS Publications)* **17**(12), 3635 (2001)
- Z. Zainal, A.J. Ali, A. Kassim, M.Z. Hussein *Sol. Energy Mater. Sol. Cells.* **79**, 125 (2003)
- G.L.S.W. Shin, Agawaneb, A.V.M.G. Gang, Moholkar, J. Moon, J.H. Kim, J.Y. Lee, *J. Alloys Comp.* **526**, 25 (2012)
- I.A. Ezenwa, *Adv. App. Sci. Res.* **3**(2), 980 (2012)
- B. Thangaraju, P. Kaliannan, *J. Phys. D* **33**, 1054 (2000)
- N. Satoa, M. Ichimuraa, E. Araia, Y. Yamazaki, *Sol. Energy Mater. Sol. Cells* **85**, 153(2005)
- P.K. Nair, M.T.S. Nair, R.A. Zingaro, E.A. Meyers, *Thin Solid Films* **239**, 85 (1994)
- N.R. Mathews, B.M. Hiran, Anaya, M.A.C. Jacome, C.A. Chavez, J.A.T. Antonio, *J. Electro chem. Soc.* **157**(3), H337 (2010)
- M. Devika, N.K. Reddy, K. Ramesh, K.R. Gunasekhar, E.S.R. Gopal, K.T.R. Reddy, *Semi cond. Sci. Tech.* **21**, 1125(2006)
- N.K. Reddy, K. Ramesh, R. Ganesan, K.T. Ramakrishna reddy, K.R. Gunasekhar, E.S.R. Gopal. *Appl. Phys. A* **83**, 133 (2006)
- P. Jain, P. Arun, *J. Semi cond* **34**(9), 093004-1-6 (2013)
- K. Hartman, J.L. Johnson, M.I. Bertoni, D. Recht, M.J. Aziz, M.A. Scarpulla, T. Buonassisi, *Thin Solid Films* **519**, 7421 (2011)
- B. Ghosh, M. Das, P. Banerjee, S. Das, *Sol. Energy Mater Sol. Cells* **92**, 1099 (2008)
- S.G. Hickey, C. Waurisch, B. Rellinghaus, A. Eychmuller. *J. Am. Chem. Soc.* **130**(45), 14978 (2008)
- B. Ghosh, M. Das, P. Banerjee, S. Das, *App. Sur. Sci.* **254**, 6436 (2008)
- H.M. Pathan, C.D. Lokhande, *Bull. Mater. Sci.* **27**(2), 85 (2004)
- B.R. Sankapal, R.S. Mane, C.D. Lokhande, *Mater. Res. Bull.* **35**, 2027 (2000)
- P. Mani, K. Manikandan, A.J. Ramya, A.I. Seelan, S.S. Zahirullah, M.S. Hameed, J.J. Prince. *Int. J. Chem. Tech. Res.* **6**(7), 3573 (2014)
- K. Manikandan, P. Mani, P.F.H. Inbaraj, S. Valli, J.J. Prince, *Int. J. Eng. Sci. Tech.* **4**(5), 2421 (2012)
- K. Manikandan, P. Mani, P.F.H. Inbaraj, T.D. Joseph, V. Thangaraj, J.J. Prince, *Indian J. Pure. Appl. Phys.* **12**, 354 (2014)
- K. Manikandan, P. Mani, C.S. Dilip, S. Valli, P.F.H. Inbaraj, J.J. Prince, *Appl. Surf. Sci.* **288**, 76 (2014)
- P. Mani, K. Manikandan, I.V. Potheher, P.F.H. Inbaraj, J.J. Prince, *J. Chem. Pharm. Sci.* **4**, 55 (2014)
- K.T.R. Reddy, N.K. Reddy, R.W. Miles, *Sol. Energy Mater. Sol. Cells* **90**(18), 3041 (2006)
- K. Manikandan, C.S. Dilip, P. Mani, J.J. Prince, *Am. J. Eng. Appl. Sci.* **8**(3), 318 (2015)
- S. Cheng, Y. He, G. Chen, E. Cho, G. Conibeer, *Coat. Tech.* **202**, 6070(2008)
- A. Ghazali, Z. Zainal, M.Z. Hussein, A. Kassim, *Sol. Energy Mater. Sol. Cells.* **55**, 237(1998)
- C. Gao, H. Shen, Z. Shen, L. Sun, *App. Surf. Sci.* **257**, 4439 (2011)
- J. Henry, K. Mohanraj, S. Kannan, S. Barathan, G. Sivakumar, *Eur. Phys. J. Appl. Phys.* **61**, 1 (2013)
- T. Petrov, I.M. Deneva, O. Chauvet, R. Nikolov, I. Denev, *J. Univ. Chem. Tech. Metal.* **47**(2), 197 (2012)
- M. Dai, J. Kwon, Y.J. Chabal, M.D. Halls, R.G. Gordon, *Mater. Res. Soc. Sympo. Proc.* **1155**, 1155 (2009)